Available online at www.sciencedirect.com
SCIENCE DIRECT
Journal of Catalysis 238 (2006) 100–110
JOURNAL OF CATALYSIS
www.elsevier.com/locate/jcat

A study of the mechanism for NO_x reduction with ethanol on γ-alumina supported silver

Young Hoon Yeom, Meijun Li, Wolfgang M.H. Sachtler, Eric Weitz *

Department of Chemistry and Institute for Environmental Catalysis, Northwestern University, Evanston, IL 60208, USA

Received 14 September 2005; revised 18 November 2005; accepted 25 November 2005

Available online 9 January 2006

Abstract

A multistep mechanism has been elucidated for the reduction of NO_x in the presence of added ethanol over Ag/γ-Al_2O_3 at 320 °C. Under these conditions, ethanol principally reacts with oxygen to form acetaldehyde. Surface acetate ions, which are formed from adsorbed acetaldehyde, react with NO_2 to yield nitromethane. Evidence is presented indicating that the aci-anion of nitromethane is an intermediate. In contrast, NO_x reduction with ethanol over Ag/γ-Al_2O_3 at 200 °C is inefficient, because surface acetate ions are much less reactive at 200 °C than at 320 °C. At 200 °C, the dominant pathway for ethanol oxidation is reaction with NO_2, producing ethyl nitrite, which decomposes into a number of products, including N_2O, which is stable under reaction conditions. On the basis of these mechanistic data, conditions can be defined under which NO_x reduction with ethanol may be viable.

Keywords: Ethanol; Ethyl nitrite; Acetaldehyde; FTIR; NO_x reduction; Nitromethane; Aci-anion of nitromethane; Reactivity of surface acetate

1. Introduction

Ethanol has been shown to be an efficient reducing agent for the selective catalytic reduction (SCR) of NO_x on Ag/γ-Al_2O_3, an alumina-supported silver catalyst [1,2]. This system has demonstrated good resistance to both water and sulfur inhibition, and NO_x conversion can exceed 80% in the temperature range 350–500 °C [1]. Ethanol is a particularly attractive additive for NO_x reduction in diesel exhaust, because it is relatively environmentally benign and can be easily blended with diesel fuel using an emulsifying agent. It can then be distilled from this mixture through "on-board" heating [1].

Ag/γ-Al_2O_3 catalysts have been widely studied because of their high activity for hydrocarbon SCR for NO_x [3–5]. Nevertheless, many questions remain regarding the details of the mechanism of operation of these catalysts. In particular, the reason for the low catalytic activity at ∼200 °C has not been identified; although low-temperature activity is highly desirable for removing NO_x from diesel exhaust.

It is known that good NO_x reduction is achieved with acetaldehyde at 200 °C over BaNa/Y and Na/Y zeolite catalysts [6–8]. Because oxidation of ethanol to acetaldehyde has been assumed to be facile, the different temperature requirements for these reductants are intriguing and provide our motivation for a study of SCR in the ethanol–Ag/γ-Al_2O_3 system. In particular, we seek to answer two interrelated questions: (1) Why is the activity of Ag/γ-Al_2O_3 for NO_x reduction with ethanol relatively low at 200 °C? and (2) Why is it so much higher at elevated temperatures? We present new data of relevance to these issues, including the chemistry by which crucial reaction intermediates are formed.

2. Experimental

Alumina-supported silver catalysts (Ag/γ-Al_2O_3, Ag 4 wt%) were prepared by impregnating γ-Al_2O_3 (Nanostructures and Amorphous Materials Inc.; 99%, 11 nm, 250 m^2/g) with an aqueous solution of silver nitrate. The samples were dried at 298 K for 4 h and calcined at 773 K for 5 h.

In situ FTIR spectra were recorded in transmission mode using a homemade IR cell and a Bio-Rad Excalibur FTS-3000 IR spectrometer equipped with a MCT detector. The homemade

* Corresponding author.
E-mail address: weitz@northwestern.edu (E. Weitz).

0021-9517/$ – see front matter
doi:10.1016/j.jcat.2005.11.036

infrared cell, described in detail previously [7], consists of a stainless steel cube with two CaF_2 windows that can be differentially pumped. Unless otherwise stated, each of the reported spectra is the result of averaging 70 scans at 4 cm^{-1} resolution under static conditions.

Typically, a small brush was used to "paint" 10–15 mg of sample, in a water slurry, onto a 1.5 × 1.5 cm tungsten grid held at 353 K. Before each experiment, the catalyst was heated in vacuum (2×10^{-6} Torr) for 3 h at 703 K, then cooled to the desired temperature. After this treatment, and before the catalyst was exposed to reactants, a spectrum of the catalyst was recorded and used as the "background" for a given experiment.

Ethyl nitrite was prepared by a standard method [9]. Sodium nitrite was allowed to react with ethanol at 0 °C while dilute sulphuric acid was added. The ethyl nitrite thus formed is poorly soluble in water (<1%) and is easily separated from the products by cooling the mixture to −10 °C. The FTIR spectrum of the ethyl nitrite sample thus obtained showed no detectable impurities.

3. Results

This work focuses on a mechanistic understanding of why the activity of the Ag/γ-Al_2O_3 catalyst for NO_x reduction with ethanol at 200 °C is relatively low and increases significantly at higher temperature. Our studies have focused on the identification of the critical intermediates in the deNO_x chemistry with ethanol over Ag/γ-Al_2O_3.

3.1. Gas-phase intermediates in the reaction of ethanol + NO_2 + O_2

Fig. 1 displays time-resolved gas-phase spectra taken after exposing Ag/γ-Al_2O_3 to a mixture of ethanol, NO_2, and O_2 at 200 °C. In this experiment the IR beam was directed through the cell to a portion of the wire grid that was not covered with the Ag/γ-Al_2O_3 sample. To minimize the reaction of ethanol with NO_2 in the gas phase, NO_2 was introduced into the IR cell before admission of a previously prepared mixture (premix) of ethanol and oxygen. The strong absorption bands at 1064 and 1616 cm^{-1}, due to ethanol and NO_2, respectively, decreased gradually with time; the ethanol band decreased by ∼45% after 27.6 s. The absorption band of NO_2 in the top trace in Fig. 1 was enhanced in intensity due to compression of gas-phase NO_2 into a portion of the IR cell when the ethanol and O_2 mixture was introduced into the cell. Therefore, the decreased intensity of the NO_2 absorption with time was due not only to reaction with ethanol, but also to diffusion of NO_2 inside the IR cell. The bands at 1671 and 1745 cm^{-1} formed and gradually increased in intensity with time. The band at 1874 cm^{-1} was due to NO, which is in equilibrium with NO_2,

$$2NO_2 \equiv 2NO + O_2.$$

The isotopically labeled compounds, ^{15}NO and $^{13}CH_3CH_2OH$, were used to help assign the absorptions at 1671 and 1745 cm^{-1} in Fig. 2. Spectrum (a) is of unlabeled "authentic" ethyl nitrite. The bands centered at 1618 cm^{-1} and 1671 are due to the N=O stretching vibrations of *cis*- and *trans*-ethyl nitrite, respectively [9]. The bands at 1671 and 1745 cm^{-1} in spectrum (b) are due to intermediates produced from the $^{13}CH_3CH_2OH + NO_2$ reaction. The bands at 1642 and 1745 cm^{-1} in spectrum (c)

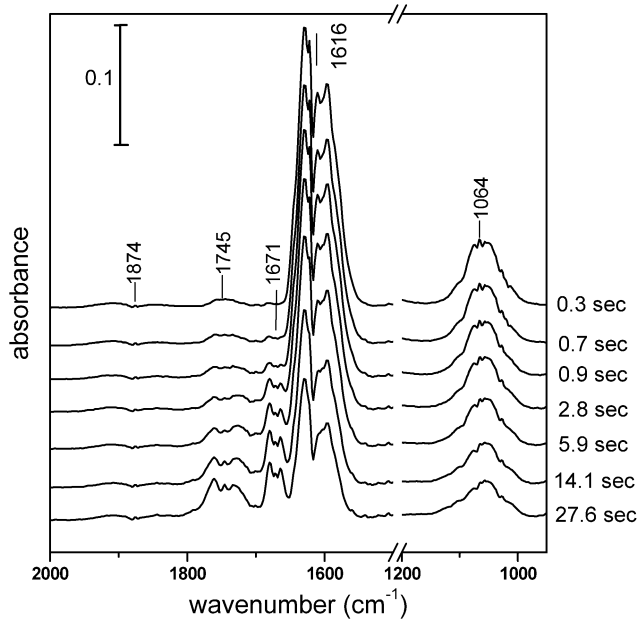

Fig. 1. Time resolved FT-IR spectra after Ag/γ-Al_2O_3 was pre-exposed to 2 Torr NO_2 and subsequently exposed to a mixture of 3.8 Torr ethanol + 60 Torr O_2 at 200 °C. Spectra were recorded immediately after introduction of the mixture.

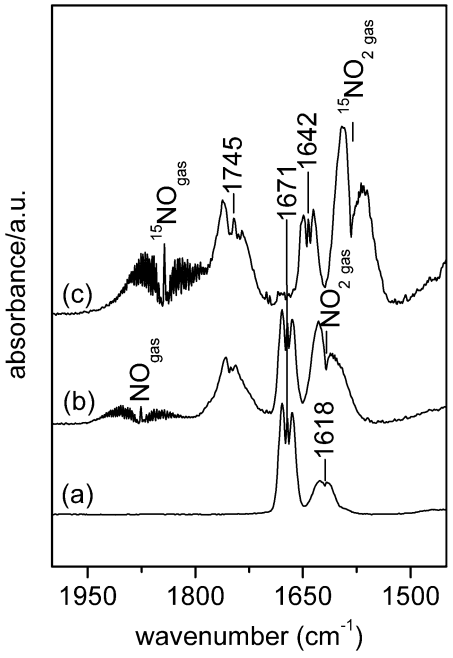

Fig. 2. Gas phase FT-IR spectra: (a) 2 Torr of ethyl nitrite at 25 °C, (b) spectrum of the gas phase over Ag/γ-Al_2O_3 after exposure of Ag/γ-Al_2O_3 to 2 Torr NO_2 + 3.8 Torr 2-^{13}C-ethanol + 60 Torr O_2, (c) Spectrum of the gas phase over Ag/γ-Al_2O_3 after exposure of Ag/γ-Al_2O_3 to 2 Torr ^{15}NO + 3.8 Torr ethanol + 60 Torr O_2. Prior to admission of the premixture of 3.8 Torr ethanol + 60 Torr O_2, the Ag/γ-Al_2O_3 was pre-exposed to 3.8 Torr of NO_2 (or ^{15}NO).

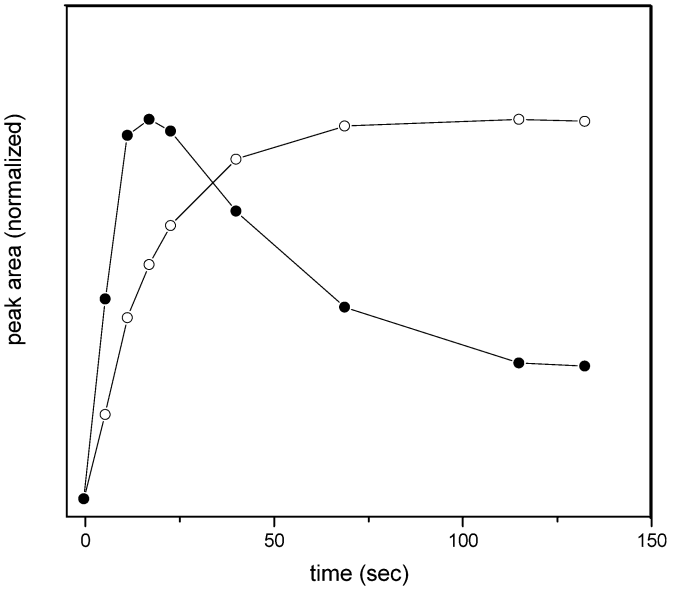

Fig. 3. The rate of ethyl nitrite formation from the reaction of ethanol and NO_2 (○) in the absence and (●) in the presence of the Ag/γ-Al_2O_3 catalyst. Ag/γ-Al_2O_3 was pre-exposed to 2 Torr NO_2 and subsequently exposed to a mixture of 3.6 Torr ethanol + 70 Torr O_2 at 200 °C. The indicated amplitude is based on an integration of the gas phase ethyl nitrite band centered at 1671 cm^{-1}.

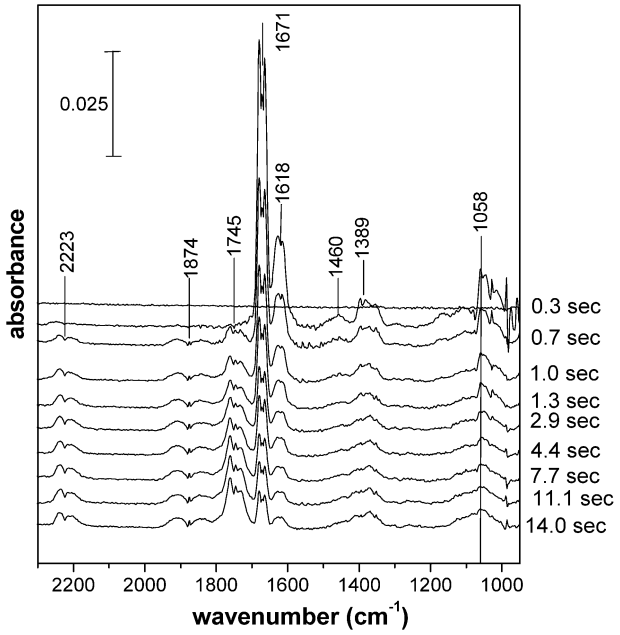

Fig. 4. Time resolved FT-IR spectra of gas phase species after exposure of Ag/γ-Al_2O_3 to 2 Torr of ethyl nitrite at 200 °C.

are due to intermediates of the reaction of ethanol with $^{15}NO_2$. The band at 1745 cm^{-1} is readily assigned to gas-phase acetaldehyde because its shape and position agree well with that of authentic gas-phase acetaldehyde (not shown) and because this band does not shift on ^{15}N labeling. The absorption at 1671 cm^{-1} did not shift when using $^{13}CH_3CH_2OH$ as the reactant (see trace (b)), but did shift to 1642 cm^{-1} when using ^{15}NO as the reactant (see trace (c)). Clearly, this band is not due to a C=C, a C=N, or a C=O stretching vibration. The band at 1671 cm^{-1} is readily assigned to the N=O stretching vibration of *trans*-ethyl nitrite. The expected positions of the N=O and ^{15}N=O stretches of *cis*-ethyl nitrite in spectra (b) and (c) are masked by the strong gas-phase bands of NO_2 and/or $^{15}NO_2$.

3.2. Ethyl nitrite formation and decomposition

Fig. 3 displays data relevant to the rates of ethyl nitrite formation from the reaction of ethanol and NO_2. It has been reported that ethanol reacts with NO_2 in the gas phase [10]. However, a comparison of the rate of ethyl nitrite formation in the gas phase, in the presence and the absence of Ag/γ-Al_2O_3, demonstrates more rapid formation of ethyl nitrite in the presence of Ag/γ-Al_2O_3. In the presence of Ag/γ-Al_2O_3, ethyl nitrite production reached a maximum after ∼16 s, whereas it took ∼120 s to reach a maximum in the absence of Ag/γ-Al_2O_3. Even more relevant is the observation that in the presence of Ag/γ-Al_2O_3, the amount of ethyl nitrite in the gas phase decreased rapidly after passing a maximum. As shown in Fig. 5, ethyl nitrite decomposed rapidly on the solid surfaces used in this study.

Fig. 4 displays time-resolved gas-phase spectra taken after exposing Ag/γ-Al_2O_3 held at 200 °C to 2 Torr of authentic ethyl nitrite. The intensity of the known bands of gas-phase ethyl nitrite at 1058, 1389, 1460, 1618, and 1671 cm^{-1} decreased rapidly with exposure time. But *adsorbed* ethyl nitrite was not detected, presumably because it rapidly decomposed on Ag/γ-Al_2O_3 under these conditions. On the other hand, the gas-phase absorption of acetaldehyde at 1745 cm^{-1} gradually increased in intensity. Ethanol was also observed at 1058 cm^{-1}. This ethanol band overlapped with a gas-phase ethyl nitrite band. A weak absorption due to gas-phase ethanol was also detected at 3675 cm^{-1} (not shown). The sharp features at 950–1030 cm^{-1} in the traces taken at 0.3 and 0.7 s are due to noise. The absorptions centered at 1874 and 2223 cm^{-1} are due to NO and N_2O, respectively. More than 80% of these compounds were formed between recording the first and second traces. Absorptions of gas-phase H_2O were not detected under these conditions, but became evident when 6 Torr of ethyl nitrite was introduced into the cell (not shown). These data reveal that the products of the gas-phase decomposition of ethyl nitrite included acetaldehyde, ethanol, NO, N_2O, and H_2O.

Table 1 displays the composition of the gas phase subsequent to decomposition of 90% of the ethyl nitrite, which corresponds to a ∼20 s reaction time. The percentages are based on calibrations of absorptions of the relevant species using authentic samples and known pressures. As discussed in more detail in Section 4.1, the overall reaction of ethyl nitrite decomposition in the absence of O_2, can be written as

$$4CH_3CH_2ONO \rightarrow 3CH_3CHO + CH_3CH_2OH + 2NO + N_2O + H_2O.$$

Note that NO_2 is not a primary product of ethyl nitrite decomposition.

It may be surprising that approximately the same amount of N_2O was observed in the absence and the presence of O_2. We

Table 1
Analysis of ethyl nitrite decomposition over $Ag/\gamma\text{-}Al_2O_3$ in the absence (left column) or in the presence of O_2 (right column)

C-containing species	*C-containing species*
Acetaldehyde 29%	Acetaldehyde 43%
Ethanol 41%	Ethanol 17%
Ethanol + acetaldehyde	Ethanol + acetaldehyde
On the surface 30%[a]	On the surface 40%[a]
N-containing species	*N-containing species*
NO 89%	NO 40%
N_2O 11%	N_2O 11%
NO_2 0%	NO_2 19%
NO_2 on the surface 0%	NO_2 on the surface 30%[a]

Note. $Ag/\gamma\text{-}Al_2O_3$ was exposed to 6 Torr of ethyl nitrite on Ag/Al_2O_3 at 200 °C. Gas phase species were analyzed after 90% of the ethyl nitrite had decomposed.

[a] The amount of surface adsorbed acetaldehyde, ethanol, and NO_2 is estimated.

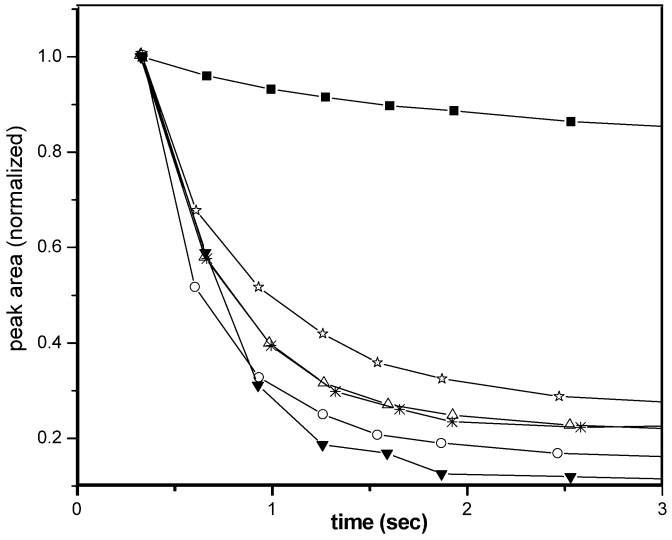

Fig. 5. Ethyl nitrite decomposition on various surfaces: SiO_2 (☆), Al_2O_3 (△), $Ag/\gamma\text{-}Al_2O_3$ (∗), H-Y (○), and Ag-Y (▼) and in the absence of a catalyst (■). The gas phase ethyl nitrite band centered at 1671 cm^{-1} was integrated to obtain amplitudes.

discuss this issue further in Section 4.1. Trace amounts of N_2O are produced when only NO_2 is introduced into the cell, holding the $Ag/\gamma\text{-}Al_2O_3$ sample at 200 °C.

Fig. 5 displays data on the kinetics of ethyl nitrite decomposition over SiO_2, $\gamma\text{-}Al_2O_3$, $Ag/\gamma\text{-}Al_2O_3$, H-Y, and Ag-Y. As shown in the top trace, ethyl nitrite was relatively stable in an IR cell containing only the tungsten mesh. However, in the presence of a metal oxide or a zeolite, the amount of ethyl nitrite decreased dramatically. This decrease was not due to mere adsorption; decomposition also occurred, as evidenced by the formation of new compounds. As mentioned earlier, ethyl nitrite was not detected on either $\gamma\text{-}Al_2O_3$ or $Ag/\gamma\text{-}Al_2O_3$ (the only systems in the foregoing list that have been studied in detail) under these conditions, because it decomposed rapidly (roughly 60% of added ethyl nitrite decomposes within ∼1 s of contacting any of the surfaces listed above) and volatile decomposition products were observed in the gas phase.

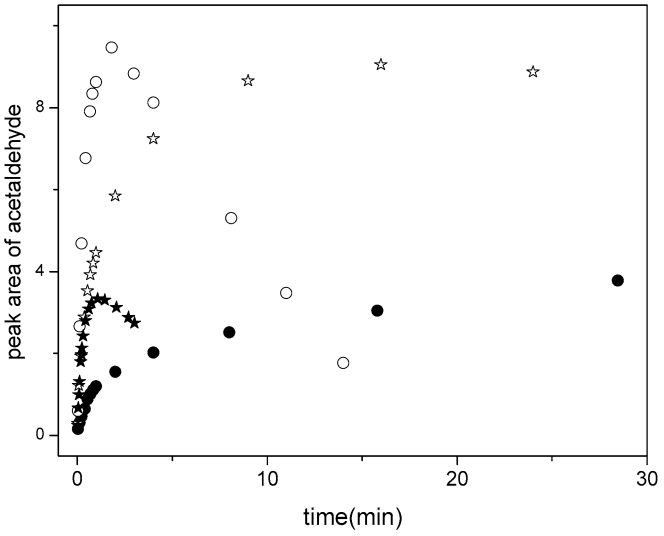

Fig. 6. The rate of acetaldehyde formation from the reactions of: (●) ethanol + O_2 at 200 °C, (☆) ethanol + NO_2 + O_2 at 200 °C, (○) ethanol + O_2 at 320 °C, and (★) ethanol + NO_2 + O_2 at 320 °C. The acetaldehyde absorption band centered at 1745 cm^{-1} was integrated to obtain amplitudes.

3.3. Acetaldehyde formation

Fig. 6 shows the result of exposing $Ag/\gamma\text{-}Al_2O_3$ to reactants at the indicated temperatures, while monitoring the formation of acetaldehyde. The trace marked by ● displays data for a premix of 3.8 Torr ethanol + 60 Torr O_2. In the trace marked by ☆, $Ag/\gamma\text{-}Al_2O_3$ was exposed first to 3.8 Torr NO_2, then to the premix. Comparing these two traces shows that the rate of acetaldehyde formation at 200 °C was higher when the surface was first exposed to NO_2. Even with no NO_2 present, acetaldehyde formation was very rapid when the temperature was increased to 320 °C. Experiments were performed to determine whether NO_2 affects the rate of acetaldehyde formation at 320 °C. The peak maximum was at ∼1.0 min in the presence of NO_2 (see the trace with ○) and 1.7 min in the absence of NO_2 (see the trace with ★). Therefore, even at 320 °C, some portion of acetaldehyde came from the oxidation of ethanol by NO_2. In the trace marked by ●, the intensity of the acetaldehyde absorption decreased gradually as acetaldehyde reacted with oxygen, as evidenced by the formation of CO_2. In the trace marked by ★, the acetaldehyde that was produced reacted rapidly with NO_2, and thus the height of the acetaldehyde peak is low relative to the traces marked by (☆) and (○), even though the rate of acetaldehyde formation was quite rapid.

We have confirmed that ethylene formation due to the dehydration of ethanol was negligible in the presence of oxygen at 200 °C. However, a small amount of ethylene formed when the catalyst temperature was increased to 320 °C.

3.4. Reactions of acetaldehyde on $Ag/\gamma\text{-}Al_2O_3$

Fig. 7 displays data for the reactions of acetaldehyde and crotonaldehyde on $Ag/\gamma\text{-}Al_2O_3$. On exposing $Ag/\gamma\text{-}Al_2O_3$ held at 37 °C (see trace (a)) to acetaldehyde, crotonaldehyde, with bands at 1670 and 1650 cm^{-1}, was formed. Surface acetate, with bands at 1575 and 1460 cm^{-1}, was also formed [7].

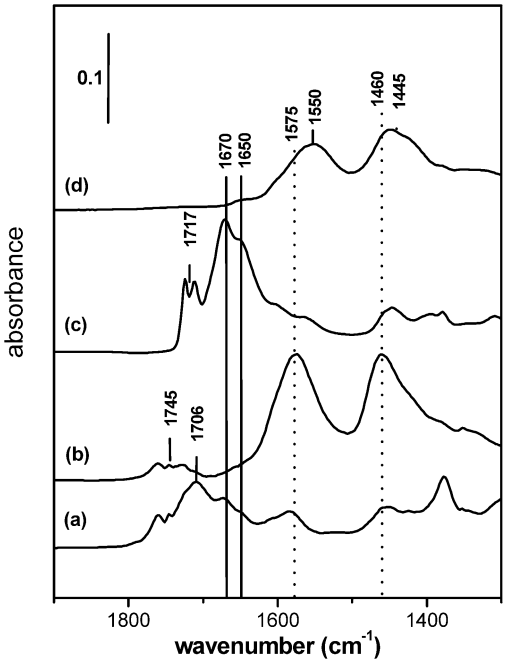

Fig. 7. (a) Ag/γ-Al_2O_3 exposed to 0.8 Torr of acetaldehyde at 37 °C, (b) the temperature is subsequently increased to 200 °C, (c) Ag/γ-Al_2O_3 exposed to 0.4 Torr of crotonaldehyde at 37 °C, (d) The temperature is subsequently increased to 200 °C. The increases in temperature were obtained with a temperature ramp of 10 °C/min.

The band centered at 1745 cm^{-1} in traces (a) and (b) is due to gas-phase acetaldehyde, and the band at 1706 cm^{-1} in trace (a) is assigned to adsorbed acetaldehyde [7]. As the temperature was increased to 200 °C, the adsorbed acetaldehyde and crotonaldehyde began to disappear and acetate bands increased in intensity (see trace (b)). After the introduction of authentic crotonaldehyde into the cell, adsorbed crotonaldehyde was observed at 1670 and 1650 cm^{-1} (see trace (c)). On further temperature increases of the Ag/γ-Al_2O_3, the bands due to adsorbed crotonaldehyde decreased in intensity, and two bands at 1445 and 1550 cm^{-1} formed (see trace (d)). These new bands are assigned to crotonate formed by crotonaldehyde oxidation on Ag/γ-Al_2O_3 [11]. A band centered at 1717 cm^{-1} is due to gas-phase crotonaldehyde. Given similar IR extinction coefficients, acetate was the major product formed on exposing Ag/Al_2O_3 to acetaldehyde at 200 °C, whereas crotonate was a minor product under these conditions.

Fig. 8 displays time-resolved spectra recorded after Ag/γ-Al_2O_3 was exposed to acetaldehyde at 200 °C. The band at 1745 cm^{-1}, due to gas-phase acetaldehyde, decreased, and acetate bands at 1578 and 1460 cm^{-1} increased rapidly with exposure time. Note that each spectrum in this figure represents one scan acquired in a 0.33-s time window. Under these conditions, surface hydroxyls were not detected, because of noise in the OH-stretching region. After exposing Ag/γ-Al_2O_3 to acetaldehyde at 50 °C in a separate experiment and averaging for 70 scans, "negative peaks" due to the loss of surface hydroxyls were observed at 3692, 3741, and 3791 cm^{-1}. Based on literature data [12], the first of these features is assigned to bridging hydroxyls, whereas the second and third bands are assigned

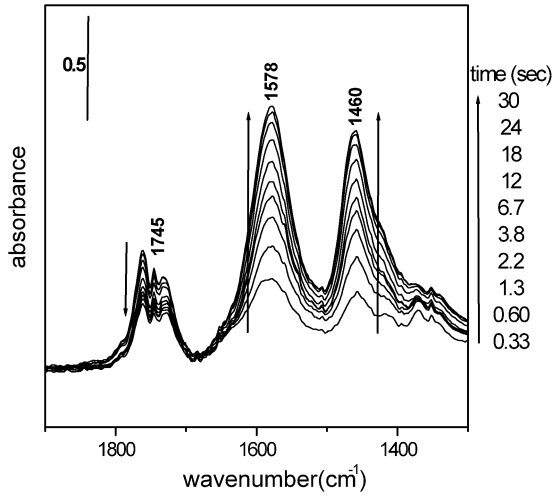

Fig. 8. Spectra recorded after Ag/γ-Al_2O_3 was exposed to 0.8 Torr of acetaldehyde at 200 °C. Each spectrum was extracted at the indicated time.

to terminal hydroxyls bound to octahedral and tetrahedral aluminum sites, respectively.

3.5. Surface species formed during NO_2 reduction with ethanol

The catalyst surface was monitored in situ during the reaction of NO_2 and ethanol over Ag/γ-Al_2O_3 at 200 °C (Fig. 9). Initially, the 1350–1800 cm^{-1} region of the spectrum in traces (a)–(e) was dominated by strong bands of gas-phase NO_2, H_2O, ethyl nitrite, and acetaldehyde. Therefore, we removed these compounds by pumping after the reaction of these species had taken place for ∼20 s at 200 °C. The remaining data in Fig. 9 were obtained after this evacuation. The absorption bands in the spectra in Fig. 9 are listed in Table 2.

The absorption bands in trace (b) match well with those in trace (a), indicating that acetate was produced. As we discuss below, surface acetate is formed from ethanol via acetaldehyde. Traces (c) and (d) are very similar, except that the band due to the symmetric stretching of acetate is shifted to 1456 cm^{-1} due to the effect of the ^{13}C methyl carbon. The acetate absorption expected at ∼1579 cm^{-1} is not visible in either trace, presumably because it is masked by the strong NO_3^- absorption at 1587 cm^{-1}. In trace (e), the absorption at 1579 cm^{-1} is due mainly to $^{15}NO_3^-$, but the acetate absorption alluded to above would be expected to contribute to this latter absorption. No N-containing moieties, such as C=N, C–NO_2, or C–ONO, are observed in this region of the spectrum. Thus, all bands observed at 1300–1800 cm^{-1} under these conditions can be assigned to either surface nitrate or surface acetate.

There is increasing evidence that nitromethane (NM) and/or its aci-anion can act as an intermediate in NO_x SCR with hydrocarbons [7]. Consequently, Ag/γ-Al_2O_3 was exposed to nitromethane and the resulting spectrum recorded. Trace Fig. 9f shows absorptions formed on exposing Ag/γ-Al_2O_3 to nitromethane at 37 °C. The absorptions at 1604 and 1623 cm^{-1} were also reported by Yamaguchi on exposing γ-Al_2O_3 to nitromethane at room temperature and were assigned to the

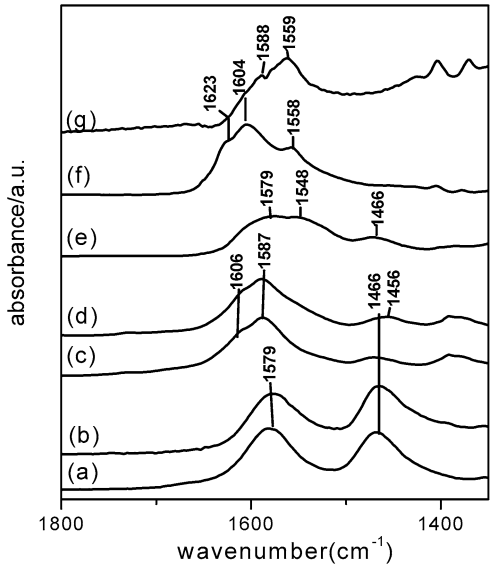

Fig. 9. Spectra of Ag/γ-Al_2O_3 exposed to: (a) acetic acid, (b) ethanol + O_2, (c) ethanol + NO_2 + O_2, (d) 2-^{13}C ethanol + NO_2 + O_2, (e) ethanol + O_2 + $^{15}NO_2$, (f) nitromethane and (g) ^{13}C-nitromethane. In each case, the cell was evacuated after 1 min of exposure to the indicated sample. The acetic acid pressure was 0.8 Torr, ethanol partial pressure was 3.8 Torr, NO_2 partial pressure was 3.8 Torr, O_2 partial pressure was 60 Torr, and nitromethane pressure was 2 Torr. The temperature was 200 °C for traces (a)–(e) and 37 °C for traces (f) and (g).

aci-anion of nitromethane ($H_2C{=}NO_2^-$), as confirmed by NMR [15]. The aci-anion of nitromethane has also been observed in studies of nitroalkanes exposed to solid oxides, including γ-Al_2O_3 [16].

With ^{13}C-nitromethane, the bands at 1623 and 1604 cm^{-1} shifted to 1588 and 1559 cm^{-1}, respectively (see trace (g)). The isotopic shift for the C=N vibration of *N*-ethylidenemethylamine ($CH_3CH{=}NCH_3$) on ^{13}C substitution was 34 cm^{-1}. This provides a plausible expectation for the isotopic shift of the aci-anion on ^{13}C substitution [17]. Likewise, the absorption at 1604 cm^{-1} shifted and overlapped with absorption due to physisorbed NM, which can be seen in trace f in Fig. 9. Thus, the higher-frequency component of the 1559 cm^{-1} absorption band is assigned to the shifted 1604 cm^{-1} absorption of the aci-anion of NM, which would be expected to be centered at ∼1570 cm^{-1}.

As discussed below, there was also a band due to ^{12}C surface formate, centered at 1604 cm^{-1}. A typical shift for a carbonyl absorption on ^{13}C substitution is ∼40 cm^{-1}, which would shift this absorption to ∼1564 cm^{-1}. Such a shift is compatible with the spectrum in trace g in Fig. 9. Thus, the absorption band centered at 1559 cm^{-1} in trace Fig. 9g has contributions from three species: the aci-anion of NM, physisorbed NM, and surface formate.

After evacuation for 20 min at 37 °C (not shown), the band at 1623 cm^{-1} in trace f in Fig. 9 decreased markedly in intensity, and the absorption at 1558 cm^{-1} was no longer visible. The band at 1604 cm^{-1} became shaper and shifted to 1590 cm^{-1}. The absorptions remaining after this treatment are assigned to surface formate. At 200 °C, the absorptions of both physisorbed nitromethane and its aci-anion were no longer visible; however, formate forms so rapidly from NM that its absorption would make identification of small amounts of the aci-anion difficult. The NCO^- ion was also observed at 2252 cm^{-1} when Ag/γ-Al_2O_3 was exposed to NM, even at temperatures as low as 100 °C.

Under reaction conditions, nitromethane and its aci-anion are reaction intermediates and thus were expected to be present at much lower concentrations than when nitromethane was introduced into the cell. Above 200 °C, nitromethane reacted very rapidly and consequently was not observed. The same was true for its aci-isomer. The aci-anion absorbs at 1604 cm^{-1}, where its band was partly masked by the surface nitrate.

3.6. Reactivity of surface acetate

Fig. 10 displays data relevant to the reactions of acetic acid on the Ag/γ-Al_2O_3 surface. Strong absorptions due to surface acetate occurred at 1460 and 1575 cm^{-1} (trace (a)). There was a broad and weak absorption at 1300–1240 cm^{-1}, which,

Table 2
Assignments for absorptions in the spectra in Fig. 9

Spectra	cm^{-1}	Adsorbed species	Assignments	Reference
(a), (b)	1466	Acetate	ν_s(O=C–O$^-$)	[13]
	1579	Acetate	ν_{as}(O=C–O$^-$)	
(c), (d)	1456 in (d)	Acetate	ν_s(O=C–O$^-$)	
	1466 in (c)	Acetate	ν_s(O=C–O$^-$)	
	1587	Bridging bidentate nitrate	ν(N=O)	[14]
	1606	Chelating bidentate nitrate	ν(N=O)	
(e)	1466	Acetate	ν_s(O=C–O$^-$)	
	1548	Bridging bidentate nitrate	ν(^{15}N=O)	
	1579	Chelating bidentate nitrate + acetate	ν(^{15}N=O) + ν_{as}(O=C–O$^-$)	
(f)	1558	Physisorbed NM	ν_{as}(NO_2)	
	1604	ac-NM + formate	ν(C=N) + ν_{as}(O=C–O$^-$)	[15]
	1623	aci-NM	ν(C=N)	
(g)	1559	Formate	ν_{as}(O=^{13}C–O$^-$)	
	1588	aci-NM + physisorbed NM + formate	ν(^{13}C=N) + ν_{as}(NO_2) + ν_{as}(O=^{13}C–O$^-$)	

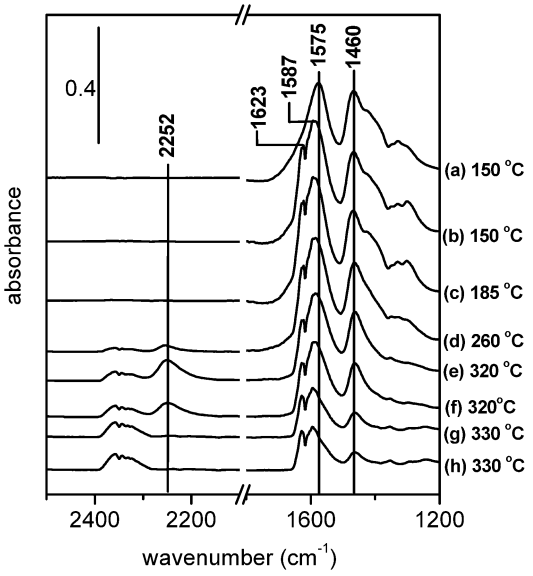

Fig. 10. Ag/γ-Al_2O_3 was exposed to 1.3 Torr acetic acid and the gas phase acetic acid was then removed by evacuation. The spectrum in (a) was recorded after evacuation. After evacuation of the acetic acid, 4.9 Torr $NO_2 + 60$ Torr O_2 was introduced at 150 °C, and the spectrum in (b) was recorded. At this point the temperature was increased at a rate of 5.7 °C/min up to 320 °C. In (c) the spectrum was recorded when the temperature reached 185 °C. (d) The spectrum was recorded when the temperature reached 260 °C. (e) The spectrum was recorded when the temperature reached 320 °C. (f) The spectrum was recorded again after 1 min at 320 °C. (g) The temperature was then ramped up to 330 °C, at a rate of 3 °C/min and a spectrum was recorded at this temperature. (h) A spectrum was recorded again after 1.5 min at 330 °C.

when expanded (not shown), revealed peaks at 1301, 1328, and 1420 cm^{-1}. These absorptions are due to the bending and deformation vibrations of the methyl group of surface acetate [13]. On introducing a mixture of NO_2 and O_2, strong absorptions at 1587 and 1623 cm^{-1}, due to the P and R branch absorptions of gas-phase NO_2, occurred. With increasing temperature, the acetate bands gradually decreased in intensity. A band at 2348 cm^{-1}, due to CO_2, began to develop at 260 °C and it increased in intensity in later traces. Between traces (a) and (h), ~90% of the initial surface acetate disappeared. The absorption at 2252 cm^{-1} is not seen until the trace at 260 °C, increased further at 320 °C, and then decreased in later traces. After exposing Ag/γ-Al_2O_3 to HNCO, a band of similar shape was observed at 2252 cm^{-1} (not shown). Weakly physisorbed HNCO on BaNa/Y that disappeared on evacuation of the cell was previously observed in this wavelength region [7]. However, in the present experiments, the absorption at 2252 cm^{-1} was stable with respect to evacuation and heating to 320 °C. Based on these observations, this absorption is assigned to the NCO^- ion rather than to physisorbed HNCO.

4. Discussion

As stated earlier, this work was motivated by two questions: (1) Why is the activity of the Ag/γ-Al_2O_3 catalyst for NO_x reduction with ethanol at 200 °C relatively low? and (2) Why is there a large increase in activity for NO_x reduction with ethanol at higher temperatures? Answering these questions requires an elucidation of the mechanism of ethanol oxidation as well as the mechanism for NO_x reduction subsequent to the formation of acetaldehyde via ethanol oxidation. This discussion focuses on delineating these mechanisms.

The intermediates formed in both of these processes provide much of the data that allow us to delineate the reaction mechanisms and provide answers to the foregoing questions. First, we discuss the identity of the intermediates in this system and the reactions that led to their formation and disappearance.

4.1. Reaction pathways for ethyl nitrite and ethanol

The detailed mechanism for the reactions of ethanol and ethyl nitrite is discussed below. Briefly, ethanol reacts with NO_2 to form ethyl nitrite, which can decompose, with acetaldehyde as one of the products. Once acetaldehyde is formed, the overall mechanism for the deNO_x chemistry is qualitatively very similar to that when acetaldehyde is the reductant initially added over BaNa/Y [7]. However, the kinetics and the energetics of some surface intermediates are different on BaNa/Y and on Ag/γ-Al_2O_3.

A second pathway for acetaldehyde production becomes dominant near 300 °C, at which point the reaction of O_2 with ethanol becomes the major pathway for acetaldehyde production. In fact, for deNO_x catalysis, formation of ethyl nitrite, which is favored at low temperature, is undesirable relative to the direct oxidation of ethanol to form acetaldehyde, because decomposition of ethyl nitrite leads to N_2O rather than to N_2. N_2O is effectively a "dead end" for deNO_x catalysis, because it is rather unreactive under typical conditions and effectively sequesters nitrogen in a "greenhouse gas" molecule rather than allowing it to be transformed into N_2. Another decomposition product of ethyl nitrite is ethanol. Thus, a cycle is possible in which ethanol reacts with NO_2 to form ethyl nitrite and ethyl nitrite decomposes, with one of the decomposition products being ethanol. In this cycle (Eqs. (5) and (6)), NO_2 is effectively converted to NO and/or N_2O. Because NO is also rather unreactive with acetaldehyde and surface acetates, it does not efficiently initiate deNO_x chemistry.

We now discuss the reactions of ethyl nitrite and ethanol in both the presence and absence of oxygen in more detail. Even in the absence of a solid surface, ethyl nitrite is formed from the reaction of ethanol and NO_2 [10], but the rate is ~2 times faster when Ag/γ-Al_2O_3 is present,

$$2NO_2 + EtOH \rightarrow EtONO + HNO_3. \quad (1)$$

One group [18] has reported that formation of HNO_3, in the gas phase is minimized when a 1:1 mixture of $NO + NO_2$ is used instead of NO_2 alone. In view of the gas-phase equilibrium of NO, NO_2, and N_2O_3, we can, therefore, write

$$2ROH + N_2O_3 \rightarrow 2RONO + H_2O. \quad (2)$$

Ethyl nitrite is expected to be formed in the gas phase by reaction (2). However, as mentioned above, its rate of formation increases in the presence of Ag/γ-Al_2O_3.

Once ethyl nitrite is formed, its decomposition is significantly accelerated in the presence of the surfaces used in this

study. This rate is faster over zeolites than over SiO_2, but because zeolites display higher surface area, we assume that the acceleration of this decomposition is not specific, but rather is common to solids with high surface areas, because acetaldehyde is known to be very effective in reducing NO_x over BaNa/Y and Na/Y at 200 °C [6,19]. Acetaldehyde is also a critical intermediate in the SCR of NO_x with ethanol over Ag/γ-Al_2O_3. Indeed, experiments by others [3a] have shown that acetaldehyde is as good a reductant as ethanol for the SCR of NO_x over Ag/γ-Al_2O_3 at temperatures above 300 °C. The role of the reaction of O_2 with ethanol is apparent in the work of Kass et al., who studied the SCR of NO_x with ethanol over an Ag/γ-Al_2O_3 catalyst [1]. Interestingly, N_2O formation was reportedly <5 ppm at ∼400 °C when using an ethanol/NO_x ratio of 3, for a NO_x concentration of ∼300 ppm [1]. Table 1 indicates that 11% was converted to N_2O (11% of $NO_x = 33$ ppm). Thus, our data suggest that if, in their work, all of the NO_x reacted with ethanol to produce ethyl nitrite, and all of the acetaldehyde was produced via ethyl nitrite decomposition, then the N_2O concentration would be > 33 ppm. Thus, a portion of the acetaldehyde must be produced via a different channel that does not produce N_2O. We will show that this channel is the direct reaction of ethanol with O_2.

At 200 °C, the rate of acetaldehyde formation from the reaction occurring in a mixture of NO_2 + ethanol + O_2 is much faster than that from the reaction of ethanol + O_2; that is, the majority of acetaldehyde comes from the formation and subsequent decomposition of ethyl nitrite. However, at 320 °C, the majority of acetaldehyde is formed over Ag/γ-Al_2O_3 from the reaction of ethanol + O_2, whereas only a minority is formed via the ethyl nitrite route (see Fig. 6).

Ferenc et al. [20] reported that the thermal decomposition of EtONO in the gas phase follows first-order kinetics between 200 and 230 °C. It has also been reported that EtONO decomposition in the gas phase involves free radicals [21], with an activation energy of 37 kcal/mol and a pre-exponential of 4.6×10^{13} s^{-1} for the decomposition process. Acetaldehyde, ethanol, NO, H_2O, and N_2O are formed as a result of the decomposition of ethyl nitrite over Ag/γ-Al_2O_3. The following reaction mechanism has been proposed previously [21]:

$$C_2H_5ONO \rightarrow C_2H_5O + NO, \quad (3)$$

$$C_2H_5O + NO \rightarrow HNO + CH_3CHO, \quad (4)$$

$$2HNO \rightarrow N_2O + H_2O, \quad (5)$$

$$C_2H_5O + NOH \rightarrow C_2H_5OH + NO. \quad (6)$$

These equations show, and Table 1 confirms, that N_2O is a product of this decomposition process. Based on the above mechanism, N_2O is formed via reaction (5) as a result of reaction of HNO radicals generated in reaction (4). These radicals can also react with C_2H_5O radicals, as in reaction (6).

In the SCR of NO_x under conditions relevant to diesel exhaust, there is an excess of O_2. Under these conditions, an additional reaction channel for C_2H_5O radicals has been identified. These radicals react with O_2 to produce HO_2 as follows:

$$C_2H_5O + O_2 \rightarrow CH_3CHO + HO_2. \quad (7)$$

It has also been reported that the HO_2 radicals subsequently react with NO to produce NO_2 [23],

$$HO_2 + NO \rightarrow NO_2 + OH. \quad (8)$$

The OH radicals that are formed can then react with ethyl nitrite, as follows:

$$OH + C_2H_5ONO \rightarrow H_2O + CH_3CHO + NO, \quad (9)$$

$$OH + C_2H_5ONO \rightarrow C_2H_5O + HONO. \quad (10)$$

The rate constants for reactions (9) and (10) are reported to be very similar [22]. Of course, NO will also react with O_2 to form NO_2. This set of reactions ((3)–(10)) can rationalize the increased amount of acetaldehyde relative to the N_2O produced when oxygen is added to the system.

In the absence of added O_2, the only pathway to acetaldehyde is via reaction (4), in which C_2H_5O reacts with NO. A coproduct of this reaction is HNO. Once HNO is formed, there is a competition with reaction (6), in which C_2H_5O reacts with HNO to form ethanol. Because in the absence of added O_2 ethanol is relatively unreactive with the components of the reaction mixture, its formation is effectively a "dead end" in the route to acetaldehyde. However, this situation changes in the presence of O_2, which will react with NO to form NO_2. Now ethanol is no longer a "dead end" for acetaldehyde production because, as shown in reaction (1), ethanol reacts with NO_2 to form ethyl nitrite. This reaction effectively "recycles" some of the ethanol back to ethyl nitrite, which can now react to form acetaldehyde, N_2O, and ethanol. In addition, as discussed above, there is a direct oxidative pathway from ethanol to acetaldehyde,

$$2C_2H_5OH + O_2 \rightarrow 2CH_3CHO + 2H_2O. \quad (11)$$

As expected, and as shown in Table 1, in such a reaction network less ethanol is produced when O_2 is present. More acetaldehyde, less ethanol, and a similar amount of N_2O can be explained by the indicated mechanism, provided that reaction (4) is significantly faster than the sum of the rates of reactions (7) and (11). Under these circumstances, ethanol is "recycled" by reaction (1), and the ethyl nitrite thus formed can decompose and provide another opportunity for formation of acetaldehyde and N_2O.

4.2. Intermediates

As discussed earlier, acetaldehyde is a product of ethanol oxidation with either NO_2 or O_2 as oxidants. We now discuss the interaction of acetaldehyde with Ag/γ-Al_2O_3.

4.2.1. Surface acetate and nitromethane formation

On exposing Ag/γ-Al_2O_3 to acetaldehyde at 200 °C, surface acetate is rapidly formed, even in the absence of added O_2. A plausible pathway for the formation of surface acetate under these conditions involves the oxidation of acetaldehyde by surface hydroxyls,

$$CH_3CHO + 2(OH) \rightarrow CH_3COO^- + H^+ + H_2O.$$

Acetate is observed at the same IR frequencies as when Ag/γ-Al_2O_3 is exposed to acetic acid. Silver is not likely to be important in acetate formation, because surface acetate is also observed by IR on exposure of γ-Al_2O_3 to acetaldehyde. The surface acetate formed from acetaldehyde is thermally stable at 200 °C and reacts slowly with either O_2 or NO_2. As we discuss further below, we believe that this slow reaction is the primary reason why Ag/γ-Al_2O_3 is relatively ineffective for NO_x reduction near 200 °C.

Surface acetate has also been observed when BaNa/Y is exposed to a mixture of acetaldehyde + O_2 + NO_2. Interestingly, for the BaNa/Y system, excessively high coverage of surface acetate leads to retardation of the deNO_x process [7]. This effect is attributed to the fact that excess acetate blocks sites that NO_2 needs to react with surface acetate. Similar behavior is compatible with the observation that acetic acid is not as good a NO_x reductant as acetaldehyde on BaNa/Y and on Ag/γ-Al_2O_3.

Once surface acetate is formed, all of our data point to a mechanism very similar to the one that is operative for BaNa/Y [7]. As discussed below, surface acetate can react with NO_2 to form nitromethane [7]. However, the surface acetate ions on Ag/γ-Al_2O_3 are less reactive toward NO_2 than those on BaNa/Y at 200 °C. With Ag/γ-Al_2O_3, the temperature must be raised to ∼320 °C to obtain efficient NO_x reduction even with acetaldehyde.

As the temperature of the Ag/γ-Al_2O_3 surface is increased above 260 °C in the presence of NO_2, the acetate band starts to diminish in intensity and an IR band of NCO^- starts to form. Further increases in temperature results in a significant decrease in the intensity of the acetate absorptions at ∼320 °C. These observations indicate that C–N bonds are formed by reaction of acetate with NO_2.

On BaNa/Y, the acetate ions are the precursors for formation of nitromethane, which is a critical intermediate in NO_x reduction in that system. As discussed in Section 3.5, surface acetate on Ag/γ-Al_2O_3 could be a precursor for the aci-anion of nitromethane: These data suggest that on Ag/γ-Al_2O_3, the aci-anion is the most stable form of nitromethane.

With BaNa/Y, there is evidence for a reaction channel that could produce nitromethane via a reaction pathway involving free radicals that operates in parallel to the pathway involving ionic surface intermediates [7]. This "radical channel" could be initiated by abstraction of a proton from acetaldehyde by NO_2. As discussed previously [7], in a zeolite environment, the acetyl radicals produced by proton abstraction are expected to decompose rapidly to form methyl radicals and CO. The reaction of methyl radicals with NO_2 then provides an additional pathway to nitromethane [23]. Although a detailed study of the product distribution for the Ag/γ-Al_2O_3 system, with acetic acid and acetaldehyde as reductants, providing evidence for the involvement of a radical channel, is beyond the scope of the current work, we have no evidence that excludes such a channel. Consistent with the possibility of the involvement of free radicals is the report by Obuchi et al. [24] that carbonaceous radicals, detected by ESR, were formed during SCR by C_3H_6 on Al_2O_3. In addition, as would be expected for a "radical channel," there is a greater CO/CO_2 ratio with acetaldehyde versus acetic acid on Ag/γ-Al_2O_3, just as there was of for these reductants on Ba/Y [7].

4.2.2. N-containing intermediates

Though surface acetate is the first intermediate formed by the interaction of acetaldehyde with Ag/γ-Al_2O_3, it is clear that intermediates containing C–N bonds are crucial for the production of N_2 in the SCR of NO_x with hydrocarbons [7]. The role of intermediates with C–N bonds is also clear in the present system. Surface NCO^-, with an IR absorption band at 2252 cm^{-1}, is a precursor for NH_3 production via the reactions

$$NCO^- + H^+ \equiv HNCO$$

and

$$HNCO + H_2O \rightarrow NH_3 + CO_2.$$

Clearly, isocyanate ions, NCO^-, must be produced as a result of the reaction of another N-containing intermediate. This is most likely nitromethane and/or its aci-anion. $H_2C{=}NO_2^-$ is a plausible precursor for NCO^-, which is readily formed even at 100 °C when the surface is exposed to nitromethane.

We also note that under actual reaction conditions, nitromethane (and its aci-anion) can be generated by reaction of surface acetate with NO_2. Further evidence for surface acetate being a precursor to NCO^- on the Ag/γ-Al_2O_3 surface is that in separate experiments (not shown), we have demonstrated that the carbon in NCO^- comes from the methyl carbon of the surface acetate species. As mentioned earlier, it is also possible that in addition to being produced as a result of reaction of surface acetate, NCO^- could also be produced by a radical pathway that would not require an acetate precursor. This could involve the following reactions:

$$CH_3CHO + NO_2 \rightarrow CH_3CO + HNO_2,$$
$$CH_3CO \rightarrow CH_3 + CO,$$

and

$$CH_3 + NO_2 \rightarrow CH_3NO_2.$$

The nitromethane thus produced can react as discussed above to produce NCO^-.

As mentioned in Section 3.5, although there is convincing evidence for nitromethane and the aci-anion of nitromethane as intermediates, because these species are very reactive they have not been observed on Ag/γ-Al_2O_3 under actual reaction conditions. In addition, under experimental conditions, adsorbed ethyl nitrite rapidly decomposes and thus is not observed by FTIR. Therefore, the only stable surface intermediates observed under reaction conditions are nitrates and acetates in the region between 1300 and 1800 cm^{-1}.

As has been pointed out previously [25], a buildup of surface nitrates can lead to decreased reactivity of a catalyst surface. However, under actual reaction conditions, NO is also present minimally because it is in equilibrium with NO_2. On BaNa/Y, NO reduces surface nitrates to surface nitrites, which are thermally more reactive at 200 °C. The decomposition of the nitrite then opens up surface sites for further reactions. Reduction of

surface nitrates by NO has also been observed in soil [26]. These examples illustrate that NO is an effective reductant for nitrates in various environments. Though NO does not reduce NO_3^- on Ag/γ-Al_2O_3 at 200 °C it seems reasonable that the presence of NO mitigates the buildup of surface nitrates on Ag/γ-Al_2O_3 at ∼300 °C and the concomitant decrease in surface reactivity that would be expected to result from such a buildup.

There are literature reports that moieties containing C–N bonds absorbing in the 1350–1800 cm^{-1} region are present on Ag/γ-Al_2O_3 and other oxide surfaces as a result of deNO_x chemistry. Sumiya et al. [3e] assigned an IR band at 1655 cm^{-1} to an N–O stretching mode of RONO formed from the reaction of $C_3H_6 + NO_x$ over Ag/γ-Al_2O_3. Kameoka et al. [3d] assigned absorptions at 1663 and 1656 cm^{-1} to R–ONO species formed from the reaction of NO_x with ethanol on Ag/γ-Al_2O_3 and Ag/TiO_2, respectively. But such species were not observed on Ag/γ-Al_2O_3 under our experimental conditions. Ethyl nitrite was not observed on the Ag/γ-Al_2O_3 surface in our work even though it was observed in the gas phase at 1671 cm^{-1}. Yu et al. [27] observed an IR band at 1633 cm^{-1} when Ag/γ-Al_2O_3 was exposed to ethanol and O_2 under steady-state conditions at 200–400 °C. They assigned this band to an enolic species (CH_2=CH–O^-) [27]. Bion et al. [3b] assigned a band at 1630 cm^{-1} to an ethyl carbonate species formed during NO_x reduction with ethanol on Ag/γ-Al_2O_3. These bands were not observed under our experimental conditions. Differences in experimental conditions, including differences in pressures used in various studies, could account for different reported observations.

Whenever possible, it is desirable to confirm assignments via isotopic labeling. Tanaka et al. [28] used isotopically labeled compounds in their study of NO reduction with propene over Pt/SiO_2. They assigned bands at 1655 and 1565 cm^{-1} to –ONO and –NO_2 vibrations, because these bands shifted by 40 and 35 cm^{-1}, respectively, after introduction of ^{15}NO. However, they observed bands in the same locations after introducing only NO_2 [28]. Bands at 1617 and 1578 cm^{-1} on WO_2–ZrO_2, assigned to surface nitrates, shifted by 38 cm^{-1} on exchange of ^{15}N for ^{14}N [29]. In addition, the isotopic shift for gas-phase ethyl nitrite on ^{15}N substitution was 29 cm^{-1}. Therefore, we believe it is possible that the bands observed in previous work [28] could be due to surface nitrate ions.

4.2.3. Surface formate and crotonaldehyde

At 37 °C, on Ag/γ-Al_2O_3, acetaldehyde was converted to both surface acetate ions and to crotonaldehyde by an aldol condensation reaction. Crotonaldehyde was oxidized at elevated temperatures to form crotonate, even in the absence of added O_2. The absorption bands of acetate and crotonate were readily distinguishable, and absorptions due to crotonaldehdye or crotonate was not observed when acetaldehyde was introduced at higher temperatures (e.g., 200 °C).

As mentioned earlier [7], aldol condensation of acetaldehyde to crotonaldehyde, followed by its polymerization, could block active sites. With Ag/γ-Al_2O_3 at temperatures at or above 200 °C, the present spectroscopic data indicate little formation of crotonaldehyde. It appears that acetate ions prevail over crotonaldehyde as the predominant surface species.

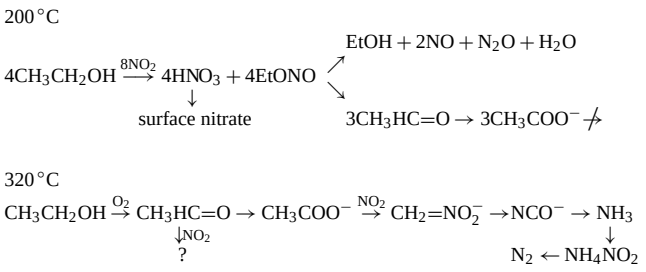

Scheme 1.

We also note that when nitromethane was adsorbed on Ag/γ-Al_2O_3 at 37 °C and the temperature of the surface is increased, formate ions, with absorptions at 1380 and 1589 cm^{-1}, were formed when the temperature reached ∼150 °C. However, we did not observe formate under actual reaction conditions. Formate is likely present at a very small steady-state concentration under actual reaction conditions. In addition, the formate absorption at 1604 cm^{-1} overlapped with the absorption of surface nitrate species, thereby masking the absorption of any formate present by the absorption of the much stronger nitrate band.

4.3. Summary of the reaction mechanism

At 200 °C, the principal oxidant for ethanol was NO_2 resulting in the formation of ethyl nitrite, the decomposition of which led to a number of products, including acetaldehyde. At 200 °C in the absence of NO_2, acetaldehyde formation was slow and surface acetate was relatively unreactive toward NO_2. Under these conditions, formation of nitromethane (and its aci-anion) was likely the rate-limiting step in the formation of ammonia and ultimately N_2 [7]. Therefore, we conclude that as with ethanol, the deNO_x activity of Ag/γ-Al_2O_3 for NO_x reduction with added acetaldehyde was very low at 200 °C.

The situation is different at 320 °C, where the yield with acetaldehyde or ethanol as primary reductants is essentially equal. At temperatures above ∼300 °C, Ag/γ-Al_2O_3 is an effective catalyst for the oxidation of ethanol with O_2 to produce acetaldehyde [30]. As discussed above, to achieve a high N_2 yield as a result of SCR of NO_x with ethanol, acetaldehyde should be formed from ethanol by oxidation with O_2. The overall mechanism is summarized in Scheme 1.

Earlier work [7] presented data indicating that dinitromethane was formed as a result of reaction of NO_2 with either nitromethane or the aci-anion of nitromethane. Although the foregoing Scheme 1 indicates that NCO^- formed from the aci-anion of nitromethane, in fact, in the absence of NO_2, nitromethane was reasonably stable at 200 °C, even though some nitromethane decomposed to form surface formate. Therefore, we believe that under actual reaction conditions, when NO_2 is present, nitromethane will react with NO_2 to form dinitromethane or, more likely, the aci-anion of dinitromethane, which can rearrange and dissociate to produce NCO^-.

5. Conclusion

Ethanol is an effective reductant for NO_x over Ag/γ-Al_2O_3 at 320 °C. The proposed mechanism for this SCR process is summarized in Scheme 1. At 320 °C, ethanol principally reacts with oxygen to form acetaldehyde. The subsequent SCR mechanism is very similar to that identified for NO_x reduction with acetaldehyde over BaNa/Y: Surface acetate ions are formed that react with NO_2 to yield nitromethane. With Ag/γ-Al_2O_3 there is evidence that the aci-anion of nitromethane is an intermediate in the deNO_x process. As with BaNa/Y, ammonia is formed by hydrolysis of NCO^- ions. This ammonia forms ammonium nitrite through reaction with $NO + NO_2 + H_2O$. This compound is thermally unstable above 100 °C and swiftly decomposes to N_2 and H_2O [31].

At 200 °C, the dominant pathway for oxidation of ethanol is reaction with NO_2. Ethyl nitrite, which is produced in this reaction decomposes into various products, including N_2O and acetaldehyde. In principle, acetaldehyde is desirable because its adsorption leads to surface acetate; however, at 200 °C, unlike in the BaNa/Y system [7], these surface acetate ions are rather unreactive. In addition, N_2O is a relatively undesirable decomposition product, because it is not reduced to N_2 under reaction conditions. Thus, nitrogen is sequestered in a "greenhouse gas" rather than being converted to environmentally benign N_2. In an actual NO_x SCR process with ethanol, most of the acetaldehyde could, in principle, be produced from ethanol oxidation by O_2, because the O_2 concentration is in excess. Thus, a plausible scheme for ethanol as a NO_x reductant is to use a catalyst that efficiently coverts ethanol to acetaldehyde via direct oxidation with O_2 at low temperatures, and then take advantage of the known efficiency for NO_x reduction with added acetaldehyde over BaNa/Y.

Acknowledgments

This work was partially supported by the Donors of the American Chemical Society Petroleum Research Fund (grant 41855-AC5) and the Chemical Sciences, Geosciences and Biosciences Division, Office of Basic Energy Sciences, Office of Science, U.S. Department of Energy (grant DE-FG02-03ER15457).

References

[1] M.D. Kass, J.F. Thomas, S.A. Lewis, J.M. Storey, N. Domingo, R.L. Graves, A. Panov, P. Park, Soc. Automot. Eng. (SAE) (2003), 01-3244.
[2] T. Noto, T. Murayama, S. Tosaka, Y. Fujiwara, Soc. Automot. Eng. (SAE) (2001) 01-1935.
[3] (a) Y. Yu, H. He, G. Feng, H. Gao, X. Yang, Appl. Catal. B 49 (2004) 159;
(b) N. Bion, J. Saussey, M. Haneda, M. Daturi, J. Catal. 217 (2003) 47;
(c) Y. Yu, H. He, Q. Feng, J. Phys. Chem. 107 (2003) 13090;
(d) S. Kameoka, Y. Ukisu, T. Miyadera, Phys. Chem. Chem. Phys. 2 (2000) 367;
(e) S. Sumiya, M. Saito, H. He, Q.-C. Feng, N. Takezawa, K. Yoshid, Catal. Lett. 50 (1998) 87.
[4] A. Keshavaraja, X. She, M. Flytzani-Stephanopoulos, Appl. Catal. 27 (2000) L1.
[5] K.-I. Shimizu, A. Satsuma, T. Hattori, Appl. Catal. B 25 (2000) 239.
[6] B. Wen, Y.H. Yeom, E. Weitz, W.M.H. Sachtler, Appl. Catal. B: Environ. 48 (2004) 125.
[7] Y.H. Yeom, B. Wen, W.M.H. Sachtler, E. Weitz, J. Phys. Chem. B 108 (2004) 5386.
[8] A. Panov, R.G. Tonkyn, M.L. Balmer, C.H.F. Peden, SAE (2001) 01-3513.
[9] P. Klaboe, D. Jones, E.R. Lippincott, Spectrochim. Acta A 23 (1967) 2957.
[10] H. Niki, P.D. Maker, C.M. Savage, L.P. Breitenach, Int. J. Chem. Kinet. 14 (1982) 1199.
[11] F. Coloma, B. Bachiller-Baeza, C.H. Rochester, J.A. Anderson, Phys. Chem. Chem. Phys. 3 (2001) 4817.
[12] C. Morterra, G. Magnacca, Catal. Today 27 (1996) 497.
[13] C. Xu, B.E. Koel, J. Chem. Phys. 102 (1995) 8158.
[14] F. Prinetto, G. Ghiotti, I. Nova, L. Lietti, E. Troconi, P. Forzatti, J. Phys. Chem. B 105 (2001) 12732.
[15] M. Yamaguchi, J. Chem. Soc., Faraday Trans. 93 (1997) 3518.
[16] P.A.J.M. Angevaare, Surface chemistry of oxygen containing compounds on oxides, Ph.D. thesis, State University of Leiden.
[17] Y. Wang, R.A. Poirier, J. Phys. Chem. A 101 (1997) 907.
[18] A.R. Doumaux, J.M. Downey, J.P. Henry, J.M. Hurt, US Patent, 4353843 (1982).
[19] S. Schmieg, B.K. Cho, S.H. Oh, Appl. Catal. B 49 (2004) 113.
[20] M. Ferenc, L. Seres, Acta Phys. Chem. 12 (1966) 35.
[21] J.B. Levy, J. Am. Chem. Soc. 78 (1956) 1780.
[22] S. Zabarnick, J. Heicklen, Int. J. Chem. Kinet. 17 (1985) 455.
[23] J.X. Zhang, J.Y. Liu, Z.S. Li, C.C. Sun, J. Comput. Chem. 26 (2005) 807.
[24] A. Obuchi, A. Ogata, K. Mizuno, A. Ohi, M. Nakamura, H. Obuchi, J. Chem. Soc., Chem. Commun. (1992) 247.
[25] Y.H. Yeom, J. Henao, M.J. Li, W.M.H. Sachtler, E. Weitz, J. Catal. 231 (2005) 181.
[26] J.M. Stark, M.K. Firestone, Soil. Sci. Am. J. 59 (1995) 844.
[27] H. He, Y. Yu, Catal. Today 100 (2005) 37.
[28] T. Tanaka, T. Okuhara, M. Misno, Appl. Catal. B Environ. 4 (1994) L1.
[29] T. Weingand, S. Kuba, K. Hadjiivanov, H. Knozinger, J. Catal. 209 (2002) 539.
[30] J.H. Lee, S.J. Schmieg, S.H. Oh, Ind. Eng. Chem. Res. 43 (2004) 6343.
[31] M. Li, J. Henao, Y. Yeom, E. Weitz, W.M.H. Sachtler, Catal. Lett. 98 (2004) 5.